DOI: 10.1002/ange.201307331

Luminescent Metal–Organic Sensors

A Luminescent Dye@MOF Platform: Emission Fingerprint Relationships of Volatile Organic Molecules**

*Ming-Jie Dong, Min Zhao, Sha Ou, Chao Zou, and Chuan-De Wu**

Abstract: *Self-assembly of luminescent moieties into porous metal–organic frameworks (MOFs) has generated many luminescent platforms for probing volatile organic molecules (VOMs). However, most of those explored thus far have only been based on the luminescence intensity of one transition, which is not efficient for probing different VOMs. We have synthesized a luminescent MOF material containing 1D nanotube channels, and further developed a luminescent dye@MOF platform to realize the probing of different VOMs by tuning the energy transfer efficiency between two different emissions. The dye@MOF platform exhibits excellent fingerprint correlation between the VOM and the emission peak-height ratio of ligand to dye moieties. The dye@MOF sensor is self-calibrating, stable, and instantaneous, thus the approach should be a very promising strategy to develop luminescent materials with unprecedented practical applications.*

As an emerging type of porous materials, metal–organic frameworks (MOFs) have the advantages over conventional inorganic porous materials in that their structures and functions are systematically and predictably designable and readily modulated.[1,2] Such unique characteristics allow for the use of MOF materials in various disciplines to realize applications in the fields of gas storage, separation, heterogeneous catalysis, photonics, and drug delivery.[3–7] Moreover, self-assembly of inorganic and organic luminescent moieties into porous MOFs has allowed us to generate unique luminescent platforms for chemical sensing, light-emitting, biotechnology, and environmental monitoring.[8] Guest-dependent luminescence sensors based on molecular coordination compounds have the distinct advantages of fast response, high sensitivity, and noninvasive operation. Although a number of luminescent MOFs have been shown to have guest-dependent optical properties, most luminescent sensors explored thus far are only based on the guest-dependent luminescence intensity of one transition, which is not accurate enough because the absolute luminescent intensity in the solid state is variable. Moreover, the probing of different volatile organic molecules (VOMs) with clearly differentiable and unique readouts based on a host MOF sensor is still a challenge, because most of this class of small molecules have similar chemical and physical properties.[9]

It has been well established that some metal ions, such as lanthanide(III) and cadmium(II) ions, can be bridged by carboxylate groups to form infinite rod-shaped metal–carboxylate secondary building units (SBUs), which have provided an effective route to construct novel MOFs with large nanotube channels.[10,11] To enhance the luminescent emission of such MOFs, we have designed and synthesized a rigid, acentric linear carboxylic ligand, (*E*)-4-(2-carboxyvinyl)benzoic acid (H_2**L**), with two chromophoric centers as a linker (Scheme 1). The solvothermal reaction of H_2**L** and $Cd(NO_3)_2{\cdot}4H_2O$ in acidified DMF solvent yielded colorless rod-like crystals of $[Cd\mathbf{L}(H_2O)]{\cdot}4DMF{\cdot}2H_2O$ (CZJ-3; CZJ = chemistry department of Zhejiang University). The formula of CZJ-3 was established based on the single-crystal X-ray structure, elemental analysis, and thermogravimetric analysis (Supporting Information, Figure S3). CZJ-3 can absorb Rhodamine B molecules into its pores to form the luminescent material Rho@CZJ-3 by taking advantage of the nanotube channels. The emission peak height of Rhodamine B in Rho@CZJ-3 can be utilized as a reference to that of the original CZJ-3 for probing small molecules. We have found that each VOM has a unique characteristic readout of the luminescent peak-height ratio between two luminescent centers in the visible light region; hence, probing different VOMs is simply realized by monitoring the relative luminescent readouts of Rho@CZJ-3.

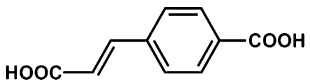

Scheme 1. (*E*)-4-(2-carboxyvinyl)benzoic acid (H_2**L**) ligand.

Single-crystal X-ray diffraction analysis revealed that CZJ-3 crystallizes in the chiral hexagonal space group $P6_522$.[12] The fundamental building unit of CZJ-3 contains one cadmium(II) cation, one **L** ligand and one coordinated water molecule. As shown in Figure 1, the two carboxylate groups of the **L** ligand comprise of two different coordination modes: the first carboxylate bridges two Cd^{II} ions in a bidentate fashion, whereas the second carboxylate chelates and bridges three Cd centers (Figure S1). The Cd cation is coordinating to six carboxyl oxygen atoms from five **L** ligands and one water molecule. The hepta-coordinated Cd^{II} ions are further bridged by carboxylate groups to form infinite 1D rod-shaped metal-carboxylate SBUs running along the *c* axis

[*] M.-J. Dong, M. Zhao, S. Ou, Dr. C. Zou, Prof. Dr. C.-D. Wu
Center for Chemistry of High-Performance and Novel Materials, Department of Chemistry, Zhejiang University
Hangzhou, 310027 (P. R. China)
E-mail: cdwu@zju.edu.cn

[**] We are grateful for the financial support of the NSF of China (21073158 and J1210042), Zhejiang Provincial Natural Science Foundation of China (Z4100038) and the Fundamental Research Funds for the Central Universities (2013FZA3006).

Supporting information for this article is available on the WWW under http://dx.doi.org/10.1002/anie.201307331.

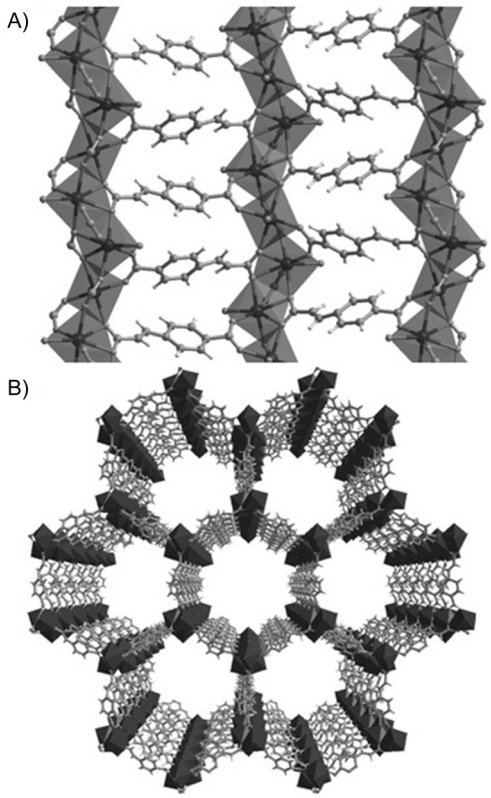

Figure 1. A) A side-view of the partial nanotube wall in CZJ-3, showing the coordination mode of **L**, the coordination environments of Cd^{II} ions, and the connection between the 1D rod-shaped Cd^{II}-carboxylate SBUs and **L** ligands. B) A perspective view of the 3D framework structure of CZJ-3 with open-ended 1D hollow chiral nanotube channels of 2 nm in diameter, as viewed along the *c* axis.

(Figure S2). Each Cd-carboxylate infinite SBU is connected with six other chains through **L** linkers to generate an interesting 3D coordination network with hexagonal nanotube channels propagated along the *c* axis. The diameter of the 1D nanotube channels is about 2.0 nm (opposite Cd···Cd distance), taking into account the van der Waals radii, in which the vacancies are filled with DMF and water molecules. PLATON calculations indicate that the vacant space in CZJ-3 is about 67.3 % of the crystal volume (2679.4 $Å^3$ of the 3982.8 $Å^3$ unit cell volume).[13]

After the as-synthesized CZJ-3 was heated at 80 °C under vacuum for 6 h, PXRD analysis of the sample showed that the sharp diffraction peaks almost disappear (Figure S4). This result suggests that CZJ-3 lost its long-range order upon removal of the included solvent molecules. However, the sharp diffraction peaks of PXRD can be restored by exposing the evacuated sample to the vapor of DMF at 80 °C for 12 h. These results suggest that the structure of CZJ-3 is flexible and reversible depending upon the solvent guests. However, such properties prevent the evaporated CZJ-3 from taking up gas molecule as confirmed by the gas adsorption experiments. Since the framework of CZJ-3 easily collapses after removal of guest solvents, we have therefore activated CZJ-3 by a solvent-exchange method (Figure S5). After the as-synthesized sample was solvent-exchanged with dry acetone several times at room temperature, a dye-uptake assay was employed to quantify the access to the pores in CZJ-3. By soaking an activated sample of CZJ-3 in an acetone solution of Rhodamine B (Figure S20; cross dimensions of ca. $6.43 \times 12.7 \times 15.5$ $Å^3$) for 24 h at room temperature, the dye was almost fully absorbed by CZJ-3, as determined by UV/Vis absorption spectroscopy, and the dye-uptake was 0.19 wt % (Figure S6). The PXRD pattern of Rho@CZJ-3, a sample embedded with Rhodamine B, suggests that the framework structure remains intact. We have also further studied the sorption abilities of CZJ-3 and Rho@CZJ-3 for different VOMs, by immersing the acetone-exchanged samples of CZJ-3 and Rho@CZJ-3 in chlorobenzene and nitrobenzene solvents for 12 h at room temperature to study their guest inclusion properties. UV/Vis analysis indicates that the activated ones readily take up 2.1 and 1.5 molecules of chlorobenzene, and 1.2 and 0.8 molecules of nitrobenzene per formula unit of CZJ-3 and Rho@CZJ-3, respectively. Rho@CZJ-3 is very stable, and the included Rhodamine B molecules cannot leak into solution during the absorption of different small solvent molecules, as determined by UV/Vis absorption spectroscopy. The above properties of Rho@CZJ-3 are beneficial for its application in sensing small molecules. To encapsulate Rhodamine B into the pores of CZJ-3, the second luminescent transition from the dye can be readily generated, in addition to the original one of the CZJ-3, whereaas the luminescent intensity ratios can be further tuned by additional solvent molecules.

The excitation and emission spectra of H_2**L**, CZJ-3 and Rho@CZJ-3 were examined at room temperature in the solid state. The free H_2**L** ligand displays an intense and broad band with a maximum at 430 nm in the emission spectrum under 310 nm UV excitation, which is attributed to the π–π^* electron transition of the H_2**L** ligand, which involves a ligand-centered excited state (Figure S10). The light emission peak of CZJ-3 shifts to 420 nm upon excitation at 340 nm (Figure S11). The blue-shift of the emission of **L** in CZJ-3 should be attributed to the deprotonation and coordination of **L** to Cd^{2+} ions.[14]

As expected, the dye encapsulated Rho@CZJ-3 simultaneously shows both the characteristic emissions of the dye and **L** moieties upon excitation at 340 nm in the solid state at room temperature. Rhodamine B and **L** within Rho@CZJ-3 emit different colors, red around 595 nm and blue around 420 nm, respectively. To make comparisons, we measured the emission spectra of Rhodamine B and a thoroughly ground mixture of Rhodamine B and CZJ-3 under the same conditions. Rhodamine B does not display any emission, whereas the mechanically ground mixture only presents the emission band of CZJ-3 excited at 340 nm in the solid-state (Figure S12). These results demonstrate that the dye molecules were encapsulated in the nanotube channels of CZJ-3, and isolation of the dye molecules by the pores of CZJ-3 can restrain the nonradiative energy transfer process, which would otherwise quench the photoluminescence.

It is interesting that such a Rho@CZJ-3 platform has allowed us to systematically tune the emissive light colors by modulating the amounts of encapsulated Rhodamine B in Rho@CZJ-3. The contents of absorbed Rhodamine B in different Rho@CZJ-3 samples were determined by UV/Vis

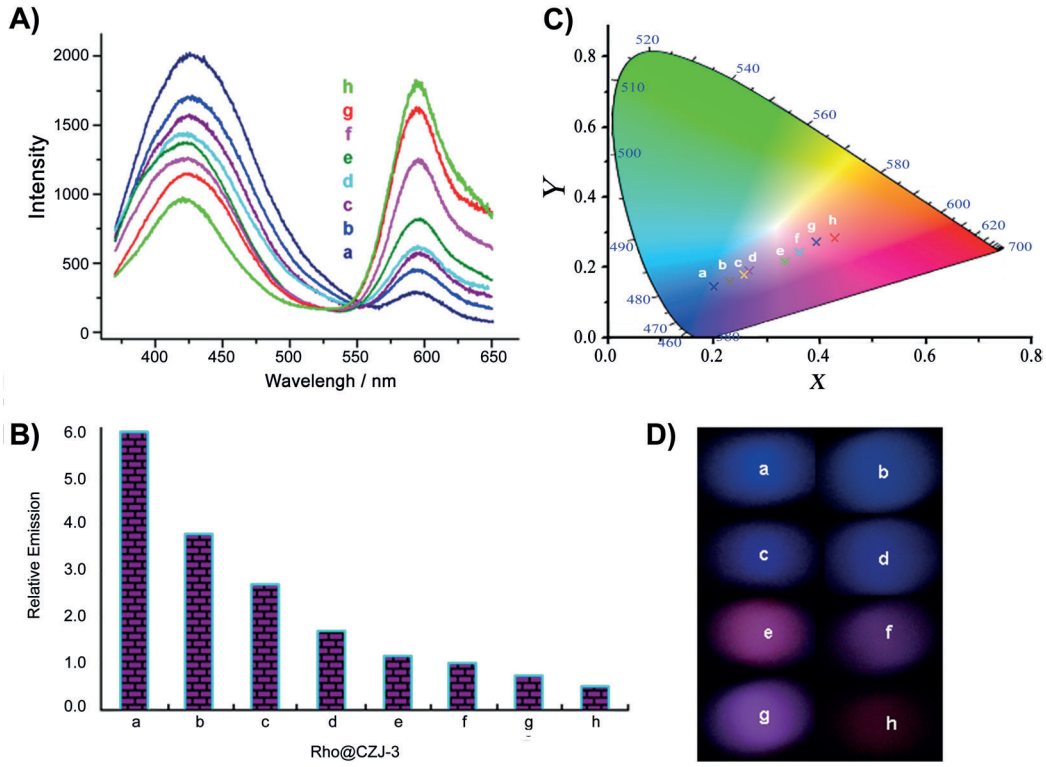

Figure 2. The emission spectra (A), emission peak-height ratios of **L** to dye moieties (B), CIE chromaticity coordinates (C), and photographs (D) with different amounts of encapsulated Rhodamine B (a = 0.02 wt%, b = 0.04 wt%, c = 0.06 wt%, d = 0.08 wt%, e = 0.1 wt%, f = 0.12 wt%, g = 0.16 wt%, and h = 0.19 wt%), for Rho@CZJ-3 excited at 340 nm in the solid-state at room temperature.

spectroscopy. As shown in Figure 2, upon increasing the Rhodamine B included in CZJ-3 (excited at 340 nm), Rho@CZJ-3 exhibits tunable emissive light colors that are controlled by decreasing the emission intensity ratio between **L** and the dye transitions. The observed emission colors of Rho@CZJ-3 match well with the calculated chromaticity coordinates, according to the 1931 Commission Internationale de L'Eclairage (CIE) chromaticity diagram, which can be clearly and directly observed with the naked eye.

The emission of the dye in Rho@CZJ-3 is mainly sensitized by the **L** moiety within the same framework. Such ligand-to-dye energy transfer behaviors have been confirmed by the emission spectra (excited at 420 nm) of the transition from the **L** moieties at room temperature (Figure S13). Moreover, the luminescence colors of Rho@CZJ-3 can be systematically modulated by tuning the excitation energy. Upon increasing the excitation wavelength, the emission intensities of **L** and dye gradually changed in the luminescence spectra of Rho@CZJ-3. These results demonstrate that the emission energy of the ligand matches well with the excitation energy of the dye. Moreover, the quantum yields of 29.5, 28.9, 28.7, 27.6, 25.4, 25.4, 23.8, and 24.3% for Rho@CZJ-3 (a–h, respectively) are higher than that of CZJ-3 (12.5%; excited at 340 nm). These values indicate that the light absorption and energy transfer balance well, which results in the enhanced luminescence of Rho@CZJ-3 from efficient ligand-to-dye energy transfer by effectively preventing the nonradiative decay.

The above results clearly demonstrate that the photoluminescent properties of Rho@CZJ-3 are variable, depending on the amounts of included Rhodamine B and the excitation energy. Additionally, as shown in Figure S21, the photoluminescence of Rho@CZJ-3 is also sensitive to the size of the MOF crystals and the homogeneity of Rhodamine B in the pores. We have used the ground samples to probe different VOMs. Because Rhodamine B is bulky, there remains enough vacant space to accommodate small solvent molecule, as demonstrated above. The induced-fit-type interaction between Rho@CZJ-3 and guest molecules will subsequently tune the energy transfer efficiency between the excited state of **L** and Rhodamine B, as the emission of the dye in Rho@CZJ-3 is mainly sensitized by the **L** moiety within the same framework excited at 340 nm. Considering that the emission peak heights of **L** and dye in Rho@CZJ-3-f are comparable, we explored its sensing capability for various VOMs by self-referencing the emission peak heights of **L** to dye moieties in the photoluminescent spectra of Rho@CZJ-3-f.

After the acetone-activated samples of Rho@CZJ-3-f were exposed to different solvents, such as 4-methylphenol, acetophenone, phenol, benzyl alcohol, and pyridine for 10 min, as shown in Figure 3 (see also Figure S14), the included solvent can be readily correlated to the emission peak heights around the 420 and 595 nm transitions in the photoluminescence spectra of Rho@CZJ-3-f. Although the emissive intensity of a single transition of **L** or dye is nonspecific to some solvents, such as acetophenone vs. phenol, these solvent molecules are easily distinguished by monitoring the emission peak-height ratios of **L** to dye moieties. Moreover, the luminescent intensities of Rho@CZJ-3 are also highly responsive to different concentrations of the mixed VOMs (Figure S22–S24). These results clearly indicate that Rho@CZJ-3 is an excellent sensor for probing different VOMs. The unique solvent-dependent emission of Rho@CZJ-3 can be rationalized by the guest-dependent energy transfer from **L** to dye moieties. Such a luminescent sensor for probing a range of solvent molecules is remarkable, because it did not require any additional calibration.

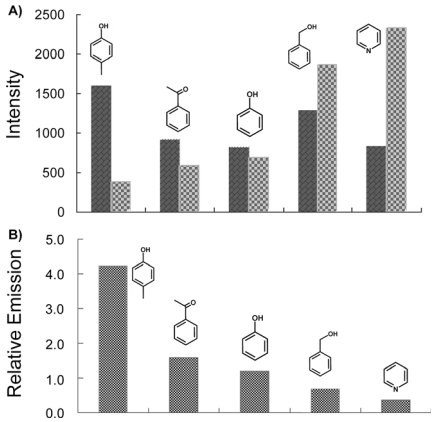

Figure 3. A) Emission peak heights of **L** (dark bars) and dye (light bars) moieties. B) The emission peak-height ratios between **L** and dye moieties in Rho@CZJ-3-f after adsorption of 4-methylphenol, acetophenone, phenol, benzyl alcohol, and pyridine molecules excited at 340 nm in the solid state at room temperature.

Above results indicate that the emission intensities of Rho@CZJ-3 are very sensitive to the included solvent molecules by tuning the energy transfer from **L** to dye moieties. The relative emission intensity of **L** versus dye moieties is almost a constant, and is unique for each guest and variable to different solvent molecules in the luminescence spectra of Rho@CZJ-3. Such characteristics can be used to draw an emission-fingerprint map of VOMs, based on the photoluminescence of Rho@CZJ-3. This internal-reference strategy should be able to overcome the drawback of variable solid-state emission intensities encountered when probing VOMs by a single emissive transition. As shown in Figure 4, even small molecules that have very similar structural motifs are unambiguously differentiable, such as isomers of *o*-, *m*-, and *p*-xylene, homologues of benzene, toluene, and ethylbenzene, and halobenzenes, including fluoro-, chloro- and bromobenzene (Figures S15–17). Although nitrobenzene and

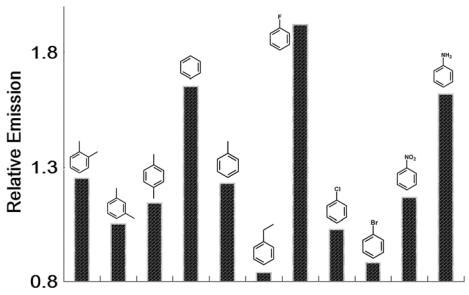

Figure 4. The solvent-dependent emission peak-height ratios of **L** to dye moieties in the luminescence spectra of Rho@CZJ-3-f excited at 340 nm in the solid state at room temperature.

aniline both exhibit significant quenching effects for the emission of Rho@CZJ-3, because of their different effects on the energy transfer from **L** to dye moieties, they are easily read-out by monitoring the relative emission peak heights of **L** to dye moieties (Figure S18).

Moreover, probing VOMs through relative emission intensity is more reliable than with absolute single-emission intensity, because the single-emission intensity is variable depending on many uncontrollable factors, whereas the peak-height ratio is almost a constant for each VOM, as observed in the luminescence spectra of Rho@CZJ-3. The sensing stability of the luminescent Rho@CZJ-3 has been shown by recycling experiments (Figure S19). Remarkably, the relative emission intensity between **L** and dye moieties in the luminescence spectra of Rho@CZJ-3-f is almost a constant for 15 cycles in sensing benzene molecules.

In summary, we have synthesized a luminescent MOF material containing 1D nanotube channels, for the first time, and developed a luminescent dye@MOF approach to realize the first dye@MOF sensor based on two emissions of host and guest for probing different VOMs. The luminescent dye@MOF platform represents a significant step forward in small molecular sensors, owing to the excellent fingerprint correlation between the solvent and emission peak-height ratio of ligand to dye moieties. Additionally, because the richness of organic linkers and dyes can be used to tune their different excited state energy in the dye@MOF platform, this very promising luminescent dye@MOF approach should be of practical use for sensitizing and probing different substrate molecules/ions by tuning the energy transfer efficiency. Such a Rho@CZJ-3 sensor is not only more stable and reliable, but also exhibits higher sensitivity than Rho@CZJ-3, based on the single-emission intensity of **L** or dye moiety. The power to unambiguously recognize VOMs highlights this approach as a very promising strategy to develop luminescent dye@MOFs with unprecedented potential applications.

Received: August 20, 2013
Revised: October 30, 2013
Published online: January 13, 2014

Keywords: fingerprint relationships · luminescence · metal-organic frameworks · relative emission · sensors

[1] For a themed issue on metal–organic frameworks, see: (Eds.: J. R. Long, O. M. Yaghi), *Chem. Soc. Rev.* **2009**, *38*, 1213.
[2] For a special issue on metal–organic frameworks, see: (Eds.: H.-C. Zhou, J. R. Long, O. M. Yaghi), *Chem. Rev.* **2012**, *112*, 673.
[3] a) G. Férey, C. Serre, T. Devic, G. Maurin, H. Jobic, P. L. Llewellyn, G. De Weireld, A. Vimont, M. Daturi, J.-S. Chang, *Chem. Soc. Rev.* **2011**, *40*, 550; b) S.-T. Zheng, T. Wu, C. Chou, A. Fuhr, P. Feng, X. Bu, *J. Am. Chem. Soc.* **2012**, *134*, 4517; c) T. A. Makal, J.-R. Li, W. Lu, H.-C. Zhou, *Chem. Soc. Rev.* **2012**, *41*, 7761; d) K. C. Stylianou, J. Rabone, S. Y. Chong, R. Heck, J. Armstrong, P. V. Wiper, K. E. Jelfs, S. Zlatogorsky, J. Bacsa, A. G. McLennan, C. P. Ireland, Y. Z. Khimyak, K. M. Thomas, D. Bradshaw, M. J. Rosseinsky, *J. Am. Chem. Soc.* **2012**, *134*, 20466.
[4] a) H. Wu, Q. Gong, D. H. Olson, J. Li, *Chem. Rev.* **2012**, *112*, 836; b) H. Deng, C. J. Doonan, H. Furukawa, R. B. Ferreira, J. Towne, C. B. Knobler, B. Wang, O. M. Yaghi, *Science* **2010**, *327*, 846; c) P. Nugent, Y. Belmabkhout, S. D. Burd, A. J. Cairns, R. Luebke, K. Forrest, T. Pham, S. Ma, B. Space, L. Wojtas, E. Mohamed, M. J. Zaworotko, *Nature* **2013**, *495*, 80; d) S. Kim, K. W. Dawson, B. S. Gelfand, J. M. Taylor, G. K. H. Shimizu, *J. Am. Chem. Soc.* **2013**, *135*, 963.

[5] a) L. Ma, C. Abney, W. Lin, *Chem. Soc. Rev.* **2009**, *38*, 1248; b) J. Lee, O. K. Farha, J. Roberts, K. A. Scheidt, S. T. Nguyen, J. T. Hupp, *Chem. Soc. Rev.* **2009**, *38*, 1450; c) A. Corma, L. I. Garcia, H. F. X. Xamena, *Chem. Rev.* **2010**, *110*, 4606; d) P. Wu, C. He, J. Wang, X. Peng, X. Li, Y. An, C. Duan, *J. Am. Chem. Soc.* **2012**, *134*, 14991; e) G.-Q. Kong, S. Ou, C. Zou, C.-D. Wu, *J. Am. Chem. Soc.* **2012**, *134*, 19851; f) A. Aijaz, A. Karkamkar, Y. J. Choi, N. Tsumori, E. Rönnebro, T. Autrey, H. Shioyama, Q. Xu, *J. Am. Chem. Soc.* **2012**, *134*, 13926; g) S. Horike, S. Shimomura, S. Kitagawa, *Nat. Chem.* **2009**, *1*, 695; h) C. Zou, Z. Zhang, X. Xu, Q. Gong, J. Li, C.-D. Wu, *J. Am. Chem. Soc.* **2012**, *134*, 87; i) X.-L. Yang, M.-H. Xie, C. Zou, Y. He, B. Chen, M. O'Keeffe, C.-D. Wu, *J. Am. Chem. Soc.* **2012**, *134*, 10638.

[6] a) Y.-Q. Lan, H.-L. Jiang, S.-L. Li, Q. Xu, *Adv. Mater.* **2011**, *23*, 5015; b) Y. Ikezoe, G. Washino, T. Uemura, S. Kitagawa, H. Matsui, *Nat. Mater.* **2012**, *11*, 1081; c) X. Kong, E. Scott, W. Ding, J. A. Mason, J. R. Long, J. A. Reimer, *J. Am. Chem. Soc.* **2012**, *134*, 14341.

[7] a) R. Vaidhyanathan, S. S. Iremonger, G. K. H. Shimizu, P. G. Boyd, S. Alavi, T. K. Woo, *Science* **2010**, *330*, 650; b) J. An, S. J. Geib, N. L. Rosi, *J. Am. Chem. Soc.* **2010**, *132*, 38; c) Y.-S. Bae, R. Q. Snurr, *Angew. Chem.* **2011**, *123*, 11790; *Angew. Chem. Int. Ed.* **2011**, *50*, 11586.

[8] a) B. Chen, S.-C. Xiang, G.-D. Qian, *Acc. Chem. Res.* **2010**, *43*, 1115; b) Y. Cui, Y. Yue, G. Qian, B. Chen, *Chem. Rev.* **2012**, *112*, 1126; c) M. D. Allendorf, C. A. Bauer, R. K. Bhakta, R. J. T. Houk, *Chem. Soc. Rev.* **2009**, *38*, 1330; d) L. E. Kreno, K. Leong, O. K. Farha, M. Allendorf, R. P. Van Duyne, J. T. Hupp, *Chem. Rev.* **2012**, *112*, 1105; e) A. Lan, K. Li, H. Wu, D. H. Olson, T. J. Emge, W. Ki, M. Hong, J. Li, *Angew. Chem.* **2009**, *121*, 2370; *Angew. Chem. Int. Ed.* **2009**, *48*, 2334; f) S. Pramanik, C. Zheng, X. Zhang, T. J. Emge, J. Li, *J. Am. Chem. Soc.* **2011**, *133*, 4153; g) N. Yanai, K. Kitayama, Y. Hijikata, H. Sato, R. Matsuda, Y. Kubota, M. Takata, M. Mizuno, T. Uemura, S. Kitagawa, *Nat. Mater.* **2011**, *10*, 787; h) K. A. White, D. A. Chengelis, K. A. Gogick, J. Stehman, N. L. Rosi, S. Petoud, *J. Am. Chem. Soc.* **2009**, *131*, 18069; i) K. C. Stylianou, R. Heck, S. Y. Chong, J. Bacsa, J. T. A. Jones, Y. Z. Khimyak, D. Bradshaw, M. J. Rosseinsky, *J. Am. Chem. Soc.* **2010**, *132*, 4119; j) Z. Xie, L. Ma, K. E. deKrafft, A. Jin, W. Lin, *J. Am. Chem. Soc.* **2010**, *132*, 922; k) H.-L. Jiang, Y. Tatsu, Z.-H. Lu, Q. Xu, *J. Am. Chem. Soc.* **2010**, *132*, 5586; l) N. B. Shustova, B. D. McCarthy, M. Dinca, *J. Am. Chem. Soc.* **2011**, *133*, 20126; m) Y. Cui, H. Xu, Y. Yue, Z. Guo, J. Yu, Z. Chen, J. Gao, Y. Yang, G. Qian, B. Chen, *J. Am. Chem. Soc.* **2012**, *134*, 3979; n) X.-L. Qi, R.-B. Lin, Q. Chen, J.-B. Lin, J.-P. Zhang, X.-M. Chen, *Chem. Sci.* **2011**, *2*, 2214.

[9] Y. Takashima, V. M. Martínez, S. Furukawa, M. Kondo, S. Shimomura, H. Uehara, M. Nakahama, K. Sugimoto, S. Kitagawa, *Nat. Commun.* **2011**, *2*, 168.

[10] P. Thanasekaran, T.-T. Luo, C.-H. Lee, K.-L. Lu, *J. Mater. Chem.* **2011**, *21*, 13140.

[11] a) Q.-R. Fang, G.-S. Zhu, Z. Jin, Y.-Y. Ji, J.-W. Ye, M. Xue, H. Yang, Y. Wang, S.-L. Qiu, *Angew. Chem.* **2007**, *119*, 6758; *Angew. Chem. Int. Ed.* **2007**, *46*, 6638; b) T.-T. Luo, H.-C. Wu, Y.-C. Jao, S.-M. Huang, T.-W. Tseng, Y.-S. Wen, G.-H. Lee, S.-M. Peng, K.-L. Lu, *Angew. Chem.* **2009**, *121*, 9625; *Angew. Chem. Int. Ed.* **2009**, *48*, 9461; c) K. Barthelet, J. Marrot, D. Riou, G. Férey, *Angew. Chem.* **2002**, *114*, 291; *Angew. Chem. Int. Ed.* **2002**, *41*, 281; d) N. L. Rosi, J. Kim, M. Eddaoudi, B. Chen, M. O'Keeffe, O. M. Yaghi, *J. Am. Chem. Soc.* **2005**, *127*, 1504; e) T. Devic, C. Serre, N. Audebrand, J. Marrot, G. Férey, *J. Am. Chem. Soc.* **2005**, *127*, 12788.

[12] Crystal data for CZJ-3: $C_{10}H_8CdO_5$, Mw = 320.56, Hexagonal, space group $P6_522$, $a = 22.4022(6)$ Å, $c = 9.1637(3)$ Å, $V = 3982.7(2)$ Å^3, $Z = 6$, $T = 293$ K, $\rho_{calcd} = 0.802$ g cm^{-3}, $\mu = 6.617$ mm^{-1}, $F(000) = 936$, 8451 reflections, 2365 independent reflections, $R_{int} = 0.0617$, $R_1[I>2\sigma(I)] = 0.0381$, $wR_2 = 0.0938$, GOF = 1.137, Flack parameter = 0.03(3). CCDC 956106 (CZJ-3) contains the supplementary crystallographic data for this paper. These data can be obtained free of charge from The Cambridge Crystallographic Data Centre via www.ccdc.cam.ac.uk/data_request/cif.

[13] A. L. Spek, *PLATON, a multipurpose crystallographic tool*, Utrecht University, Utrecht, The Netherlands, **2008**.

[14] J. R. Lakowicz, *Principles of Fluorescence Spectroscopy*, 3rd ed., Springer, Berlin, **2006**.

